 FDMP, vol.7, no.3, pp.259-278, 2011

Modeling and Simulation of Sealing Spray Application Using Smoothed Particle Hydrodynamics

Robert Rundqvist[1], **Andreas Mark**[1], **Fredrik Edelvik**[1]
Johan S. Carlsson[1]

Abstract: Multiphase flow simulation using Smoothed Particle Hydrodynamics (SPH) has gained interest during recent years, mostly due to the inherent flexibility of the method and the physically rather intuitive formulation of extra constitutive equations needed when dealing with for instance non-Newtonian flows. In the work presented here, simulations based on an SPH model implemented in the flow solver IBOFlow has been used for simulation of robotic application of sealing material on a car body. Application of sealing materials is done in order to prevent water leakage into cavities of the body, and to reduce noise. In off-line programming of the robots in the automotive paintshop it is of great interest to predict shape and appearance of sealing material without having to resort to trial and error procedures.
The flow of sealing material in the air between applicator and target (car body) is relatively uncomplicated, as the material mostly moves at constant velocity until impact on target. The flow of the material on the target is however more complex, applied material flows at the target surface due to inertia, gravity and pressure and in order to predict the appearance of the applied material, flow equations for a non-Newtonian fluid with an open surface needs to be solved. The sealing material is both thixotropic and viscoelastic; the material is shear thinning but needs to be sheared for some time before the structure of the material is broken down. Conversely, the regain of structure of the material, and thereby also the increase of viscosity when shearing is stopped or reduced, is also connected to a delay time. In the model used, the local viscosity is considered obeying a first order differential equation where the stationary limit is determined by a Bingham relation.
The simulation model was built by comparing simulations and experiments at three different stages of complexity. In the most fundamental stage the material properties were determined. Using a rotational rheometer, yield stress, plastic viscosity and thixotropy time constant was determined and implemented in the simulation model. To verify the numerical behaviour of the rheology, simulated rheometer

[1] Fraunhofer Chalmers Research Centre, Chalmers Science Park, SE-412 88 Göteborg, Sweden

experiments were carried out and compared with the physical experiments. In the second stage, simulation of application of sealing material with a stationary hollowcone nozzle was carried out. To verify the simulations, the resulting thickness, width and shape of applied material as a function of time were compared to experiments. In the third stage a moving applicator of the same type was considered, here thickness width and shape of applied material as a function of applicator to target distances were compared between experiments and simulations. At all three stages the number of SPH particles, *i.e.* grid points, in the simulations was varied in order to verify that the simulations were resolution independent.
Results of the simulations show good agreement between experiments and simulations in all stages using no artificial tuning of the models, i.e. all parameters used in the models are based on physical considerations. Furthermore, simulation time on a desktop computer indicates that computational power required for industrially relevant cases is not prohibitively large, for the most complex cases in this work the simulation time did not exceed six hours.

Keywords: Viscoelastic fluids, Thixotropy, Smoothed Particle Hydrodynamics, Free surface flow, Car body sealing

Nomenclature

D	Characteristic length scale (m)
g	Gravitational acceleration (m s^{-2})
h	Kernel smoothing length (m)
M	SPH node mass (kg)
N	Total number of SPH nodes
P	Pressure (Pa)
q	SPH distance function (m)
Δt	Time step (s)
t	Time (s)
T	Characteristic time scale (s)
u	Velocity (m s^{-1})
U	Characteristic velocity (m s^{-1})
W	Kernel weight function (m^{-3})
x	Position (m)

Greek letters

ϕ	Arbitrary field variable (-)
γ	Surface tension (N m^{-1})

$\dot{\gamma}$ Rate of deformation (s^{-1})
μ Dynamic viscosity (Pa s)
ρ Density (kg m^{-3})
τ Shear stress (Pa)

Subscripts

* Intermediate value
∞ Asymptotic value
i SPH node number
thix Thixotropic
yield Yield value

1 Introduction

Sealing material is applied to car bodies in seams to protect the car from moisture, water leakage or to dampen noice. The application, which is performed by robots, typically takes place after the body-in-white has been treated with Phosfate and Electrocoat dips, but before the different paint layers (Primer, Base coat, Top coat/Clear coat) are applied. An example of a sealing seam on a body-in-white can be seen in Figure 1.

It is of great interest to get an a priori prediction of how well the applied sealing material covers the intended regions; when commencing the production of new car models it is presently necessary to manually program the robots for new application paths in a time-consuming trial-and-error procedure. With a simulation tool able to make predictions of sealing material application and flow it would be possible both to program the robots beforehand (off-line programming) and also to be able to reduce material waste.

The sealing applicator investigated in this work is a so called hollowcone nozzle, in which a conical curtain of sealing material is sprayed onto the target. The material is broken up into droplets with a size less than a millimetre in the applicator or just downstream of it. The interaction between material droplets and air is normally negligible; the computational challenge starts as the droplets impact the target, transferring its momentum to the string that is being formed on the surface. The sealing material is non-Newtonian, the viscosity decays with increasing shear, and thixotropic – meaning that there is a certain time-lag connected to the change of viscosity. This time-lag is due to the internal breakdown and build-up of the intermolecular connections that gives the material its viscous structure. To accu-

Figure 1: Sealing material as applied to a car body.

rately model the thixotropic nature of the flow and to simplify the tracking of the free surfaces a Lagrangean method is preferred.

The simulations in this work are based on Smoothed Particle Hydrodynamics, a fluid-following method that automatically includes transport of history dependent fluid properties and propagation of a fluid/surrounding (liquid/air) interface. The principle behind the discretization concept in SPH is that the function values in the PDEs are expressed as weighted averages of the closest nodes using a smoothing kernel. In this way a continuous function approximating the solution is obtained on a discretized network in which the computational nodes are advected with the fluid velocity.

To provide the simulation with data on the physical parameters of the used sealing material experiments were preformed in a rotary rheometer. The material used is Betaguard, a PVC sealer commonly used in car industry. To quantify the inlet conditions from the applicator in use a test series with a stationary applicator was performed and to verify the simulations a number of test plates with straight strings

of material were produced.

The simulation models are currently implemented as a demonstrator module in the FCC software IPS Virtual Paint cf homepage (2011), in which the user can import geometry descriptions, define robot paths and applicator operating conditions. Results in terms of sealing material on the included geometries are displayed as the simulation progresses.

2 Experimental set-up

The experiments were carried out at Volvo Cars in Torslanda, Göteborg. In the first set of experiments, the rheology of the material used was determined. Using a rotary rheometer with a parallel disc, relations between applied torque and deformation was determined. As the sealing material was expected to exhibit thixotropic properties, the material was subjected to a series of constant deformation of successively higher rate. When the maximum rate of deformation, 450 reciprocal seconds, had been reached, the same levels were measured once more but going in the other direction – thereby it becomes possible to detect differences in timescale for internal build-up and breakdown of material structure. The setting for shear rate used in the experiments is shown in Figure 2.

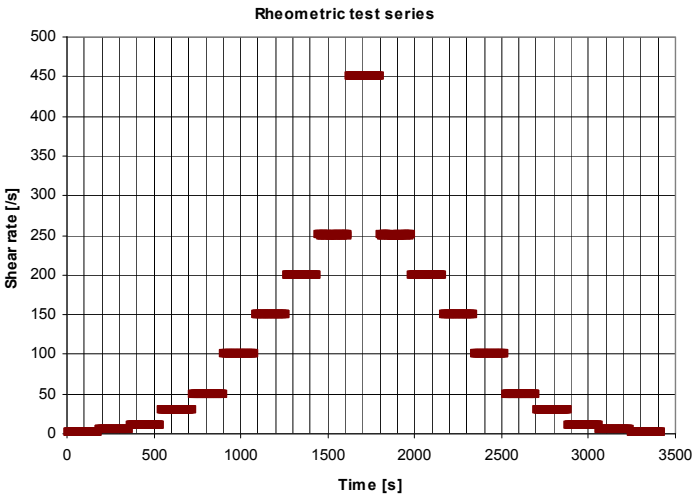

Figure 2: Rheometer deformation rate setting as a function of time.

A second set of experiments was set up in order to characterize the sealing applica-

tor studied, that is – to determine material flow rate and inlet velocities. The setup is shown in action in Figure 3.

Figure 3: Hollowcone application with a static nozzle.

Here sealing material was applied to a flat plate using a fixed hollowcone nozzle. The amount of sealing material and distance from applicator to target was varied, and the buildup of material on the target was recorded. The velocity of the material leaving the nozzle was estimated using a high speed camera and the mass flow of material at a given applicator setting was determined using a simple bucket and stopwatch approach. In the default setting used, the flow rate of material was 28.5 g/s and the density of the sealing material at ambient conditions was 1080 kg/m^3.

In a third set of experiments the applicator was allowed to move in a direction parallel to the target plate, as is shown in Figure 4. The distance between applicator and target plate was varied for different test runs, ranging from 20 to 60 millimeters, and the width of the applied strings of material was measured to be used for comparison with the simulations.

3 Numerical method

The SPH type of discretization has gained in popularity the last decade. The method has its origins in astrophysics and to some extent in computer graphics, but with recent improvements and extensions by for instance Ellero and Tanner (2005), Fang et al. (2009) and Rafiee et al (2007), the method has become increasingly useful to

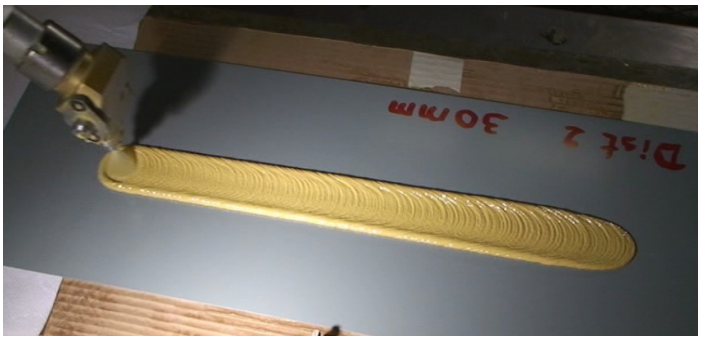

Figure 4: String application of sealing material onto a flat plate – in the image the applicator moves from right to left with a constant velocity. Distance between nozzle and target is 30 mm.

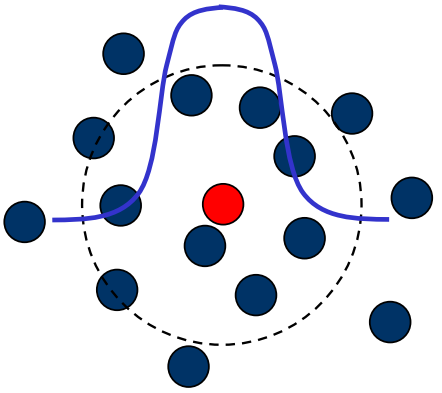

Figure 5: SPH principles. A field variable is to be evaluated by the position of the red SPH particle in the figure. Using the smoothing kernel, the value will be averaged using the nearest neighbours.

study free surface flows of general fluids. A comprehensible review of the method is given by Monaghan (2005). The SPH implementation in this paper is mostly based on the work of Cummins (1999), but with the extension to an implicit formulation of the momentum equations in order to handle the high viscosity correctly and to be able to take longer time steps. Field variables are in principle evaluated in a point by averaging the values of the surrounding nodes, weighted by the smoothing kernel. The principle is illustrated in Figure 5 and the evaluation of a variable

ϕ at a point x using a cubic spline kernel is shown in equation (1).

$$\begin{aligned}
\phi(\mathbf{x}) &= \sum_{i=1}^{N} \frac{M_i}{\rho(\mathbf{x})} \phi_i(\mathbf{x}) W_i(\mathbf{x}) \\
W_i &= \frac{1}{4h^3\pi} \begin{cases} (2-q)^3 - 4(1-q)^3, & 0 \le q \le 1 \\ (2-q)^3, & 1 < q \le 2 \\ 0, & q > 2 \end{cases} \\
q &= |\mathbf{x} - \mathbf{x}_i| / h
\end{aligned} \tag{1}$$

Here, h is the smoothing length determining the support of the smoothing kernel. Starting from Navier-Stoke's equations in the form given in equation (2),

$$\begin{aligned}
&\nabla \cdot \mathbf{u} = \mathbf{0} \\
&\frac{\partial \mathbf{u}}{\partial t} + \mathbf{u} \cdot \nabla \mathbf{u} = -\frac{\nabla \rho}{\rho} + \frac{\mu}{\rho} \nabla^2 \mathbf{u} + \mathbf{g}
\end{aligned} \tag{2}$$

the momentum and pressure equations are solved using a predictor-corrector scheme similar to the two-step projection method of Chorin (1968) First the intermediate velocities of the SPH nodes are calculated by solving the momentum equations with the pressure gradient set to zero:

$$u_{*i} - \left(\frac{\mu \nabla^2 \mathbf{u}_{*i}}{\rho_i} \right) \Delta t = u_i + g \Delta t \tag{3}$$

Note that the discretization of this equation, specifically the stress tensor which is expressed using the SPH formalism outlined in equation (1), is treated implicitly in order to handle the high viscosities in the system with a reasonable time-step. From the solution of the linearized system we get an intermediate velocity and an intermediate density. The next step is to find the pressure gradient of the next time-step by solving equation (4), in order to generate a solution field with constant density.

$$\nabla . \left(-\frac{1}{\rho_{\phi_i}} \nabla P(t + \Delta t) \right) = \frac{\rho_i - \rho_{\phi_i}}{\rho_i \Delta t^2} \tag{4}$$

Again, the gradients in the equation are evaluated according to SPH principles. In other methods, the velocity field is projected onto a divergence-free field, which is analogous to the projection to obtain constant density used here. Finally, the velocity field is projected to a solution with a constant density field:

$$u_i(t + \Delta t) = u_{\phi_i} - \frac{1}{\rho_{\phi_i}} \nabla P(t + \Delta t) \tag{5}$$

Since the method is Lagrangean by nature it is straightforward to allow for non-Newtonian liquids with thixotropy – all computational nodes move around with fluid velocity and can thus carry their own history. In the experiments it was found that the sealing material studied behaved like a Bingham fluid, that is, that the apparent viscosity of the material could be expressed as the quotient of excess shear stress to the local rate of deformation of the material, like:

$$\mu_{\infty i} = \max(0, \frac{\|\tau_i\| - \tau_{yield}}{\|\dot{\gamma}_i\|}) \tag{6}$$

at least in the stationary limit. The theory of this type of material response to stress was first developed by Eugene Bingham and a good description of the dynamics of plastic fluids can be still be enjoyed in his textbook from 1922. It should be noted that in a general flow scenario it can be numerically troublesome that the apparent viscosity goes to zero as the rate of deformation goes to infinity. However, in the case of a fixed velocity / mass flow inlet the rate of deformation will for all practical purposes be bounded by the maximum droplet momentum and the smoothing length.

For the transient part of the dynamics it is assumed that the material is of first order, obeying a simple ODE, where the transient viscosity adapts to the stationary limit according to a thixotropic timescale. In other words:

$$\frac{\partial \mu_i}{\partial t} = \frac{\mu_{\infty i} - \mu_i}{T_{thix}} \tag{7}$$

4 Results and discussion

The implementation of the method has been validated in two different transient test cases. In the Couette flow the momentum transport of the numerical implementation is verified by simulating the flow between two parallel walls of which the upper is set into constant motion at time t=0. The development of the velocity profile is shown in Figure 6. As no turbulence model has been implemented the Reynolds number is kept low.

The behaviour of the pressure solver and of the inertial properties of the flow is checked using a transient simulation of a dam break. Here a rectangular block of fluid on top of an impermeable wall is released and subjected to gravity. As the block of fluid is spread out on the surface the position of leading edge is tracked and the movement of this point is used as the basis for comparison with literature, cf Figure 7.

In both cases, a good agreement is observed between our and earlier published results. Taken together, the two test cases include effects of momentum and mass

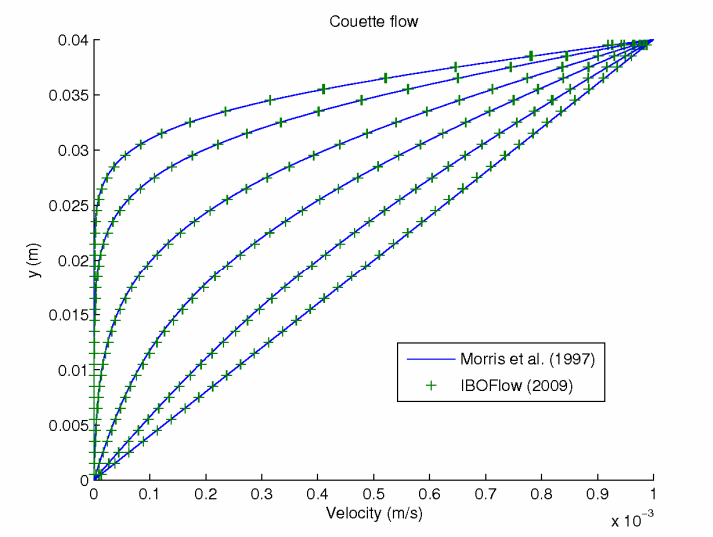

Figure 6: Comparison between results from the implemented solver (IBOFlow) and those of Morris et. al (1997). The curves represent the transient development of the velocity profile in a Couette flow. Timestep of the solver was 1.0e-3 s and the profiles in the comparison was recorded at 0.05 s, 0.1 s, 0.25 s, 0.5 s, 1.0 s and 5.0 s respectively. The Reynolds number was 0.133.

transfer driven by both gravity and pressure drop and can be considered a fairly complete test of the included discretized equations.

Simulations were set up to resemble the three different experimental setups; rotary rheometer, stationary applicator and moving applicator. In order to numerically duplicate the rheology experiments a flat cylinder of SPH particles was set up between two walls. The boundary condition with respect to the top wall was set to the rotational speed as specified in the rheometer experiment; the lower wall boundary was kept fixed. In order to compute the torque in the case of the rotary rheometer an integration of the torques from the top layer of the SPH particles were calculated. As the shear stress in the material increase with radial position, the applied torque will represent an averaging of the apparent viscosity of the SPH nodes or the material. Hence it is not trivial to obtain a correspondence between experiments and simulations.

In the stationary applicator simulation, SPH particles were injected with velocity and direction towards the target plate according to the corresponding measurements. Material properties were taken from the numerical and physical experiments

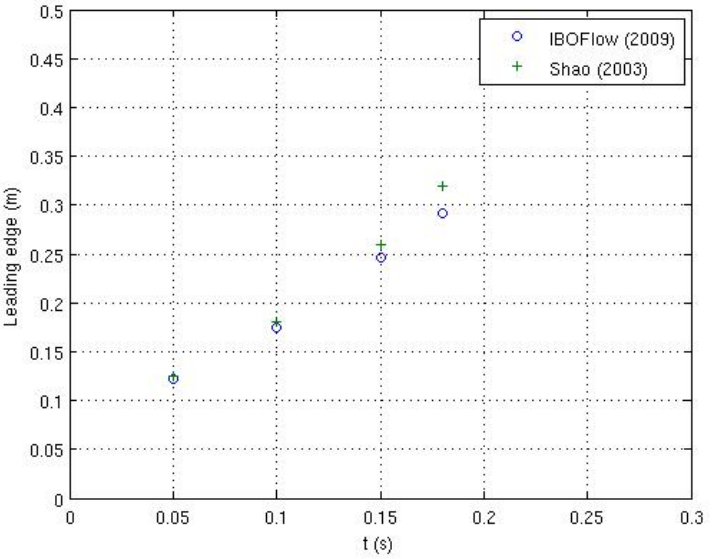

Figure 7: Comparison of the position of the leading edge of a 2D dam break as a function of time, between results from the implemented solver (IBOFlow) and those of Shao (2003).

of the rotary rheometer. As the time-scale in the impact of sealing droplets is so short in comparison to the other time-scales of the flow, this process could not be resolved and it was therefore necessary to introduce an impact coefficient of restitution between impacting SPH material and wall boundaries.

The same inlet conditions, boundary conditions and material properties are used for the simulations of the moving applicator. In order to keep memory requirements reasonable, SPH droplets were frozen after 1.0 s, which was considered long enough for the flow to settle – with an the applicator moving at a velocity of 250 mm/s and cone diameter at point of impact of maximum 40 mm, the direct flow from the applicator itself will have passed any position along its trajectory after less than 0.1 s, leaving 0.9 s for the flow to settle before the droplet is frozen.

From the rotary rheometer experiments, yield stress, Bingham plastic viscosity and structure modification time-scales were determined. Apparent viscosity as a function of time is shown in Figure 8 and the stationary shear stress is plotted versus rate of deformation in Figure 9.

In Figure 10, the different transients as response to the stepwise changes in settings

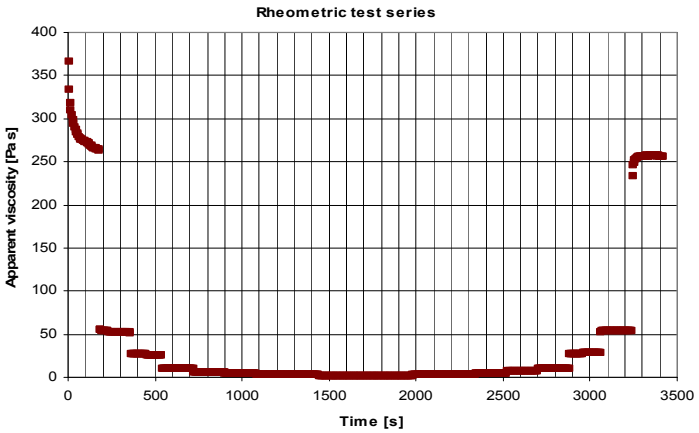

Figure 8: Apparent viscosity as a function of time, following the stepwise change in shear rate shown in Figure 3.

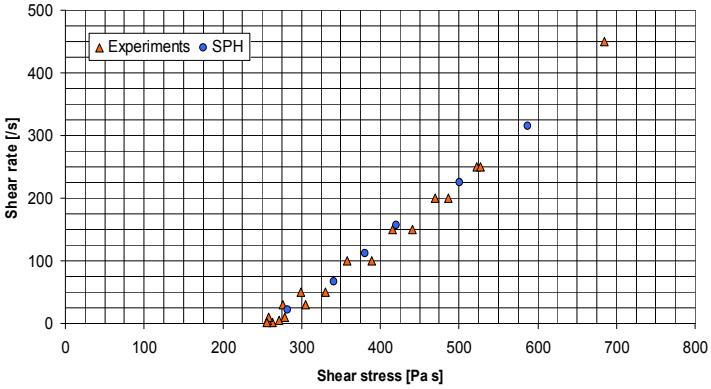

Figure 9: Stationary shear stress as computed from applied torque on rheometer versus rate of deformation, rheometer experiments (red triangles) and numerical results (blue circles).

are shown normalized in the same plot. For the higher rates of deformation the difference in viscosity was too small to reliably resolve in this analysis, so only rates of deformation up to 50 s^{-1} could be used in determining the structure adaptation time-scale. The rates of deformation in the actual material can be estimated using

impact velocity and string thickness as:

$$\dot{\gamma} \approx \frac{U}{D} \tag{8}$$

With characteristic tangential velocity U $\sim$ 1 m/s and sealing film thickness D $\sim$ 1 mm the rate of deformation at the points of impact can thus be as high as 1000 s^{-1}, but only for very short periods of time.

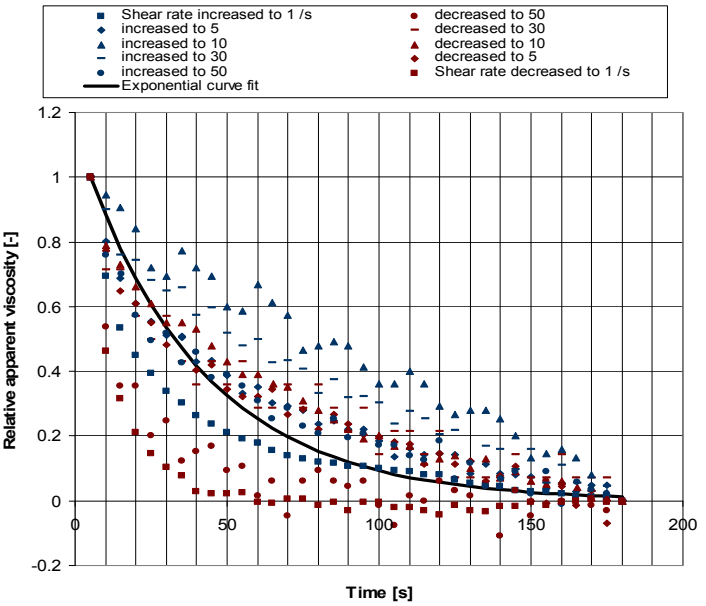

Figure 10: Rheology transients. The average time scale for viscosity adaptation estimated to 40 s.

As can be seen in Figure 10, the shape of the transients does not conform well to the first order exponential curve, meaning that the first order assumption for the transient may be questioned. On the other hand, as the estimated thixotropic time-scale of around 40 seconds is rather long compared to the other time-scales in the flow simulations the assumption still has some merit. The changes in viscosity during the passage of the applicator are nevertheless large enough to have an impact on the simulation result. In numerical experiments using a fixed viscosity instead of the first order assumption it has not been possible to reproduce features like walls and impact ditches seen in both experiments and the more advanced simulations.

A simulation of the rheometer experiment was first set up and run to verify that the fundamental models of the material rheology did give the expected results. In the

following simulations, a hollowcone nozzle was implemented. The first simulations using this nozzle were made to duplicate the experiments with the stationary nozzle and to verify the physics of sealing material impacting the plates.

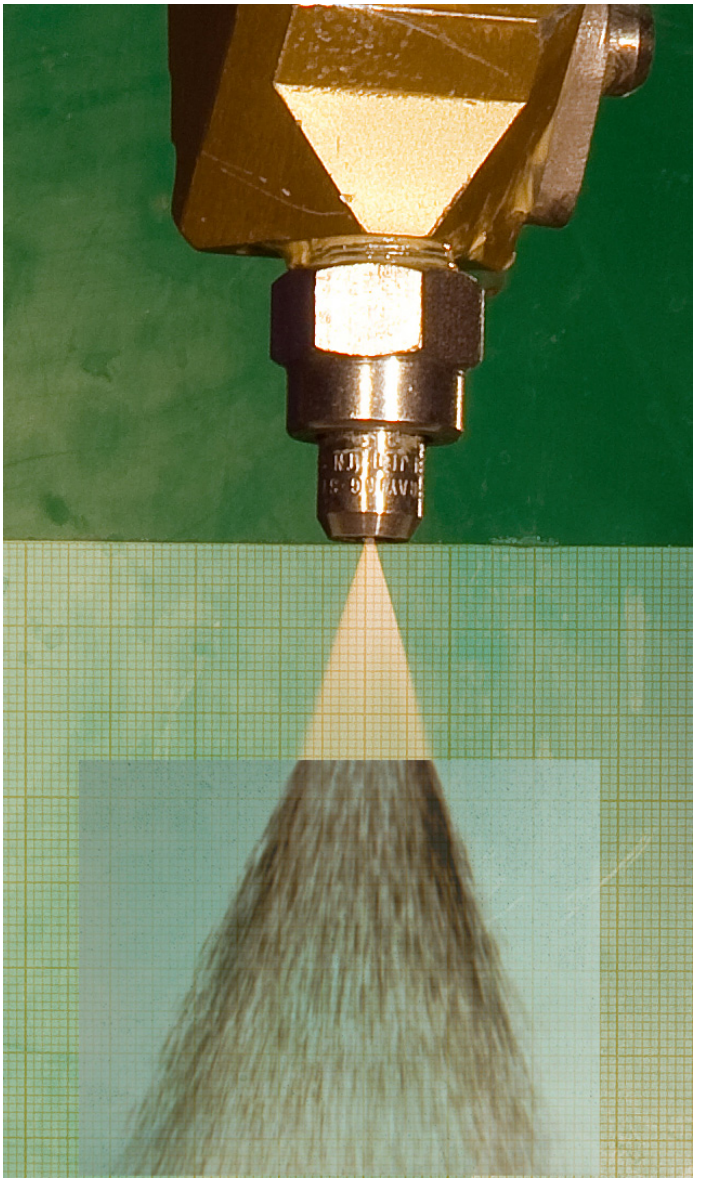

Figure 11: Stationary applicator with sealing droplets visible. Millimeter scale in the background.

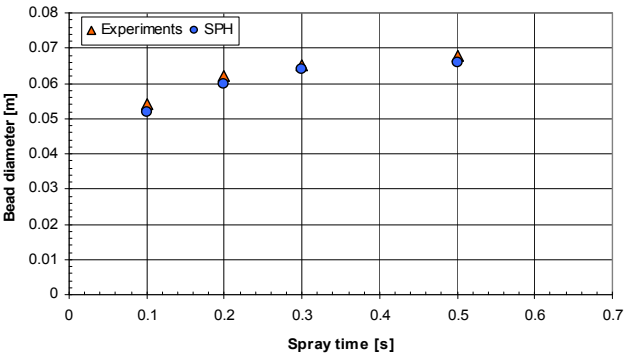

Figure 12: Bead width versus time, stationary applicator.

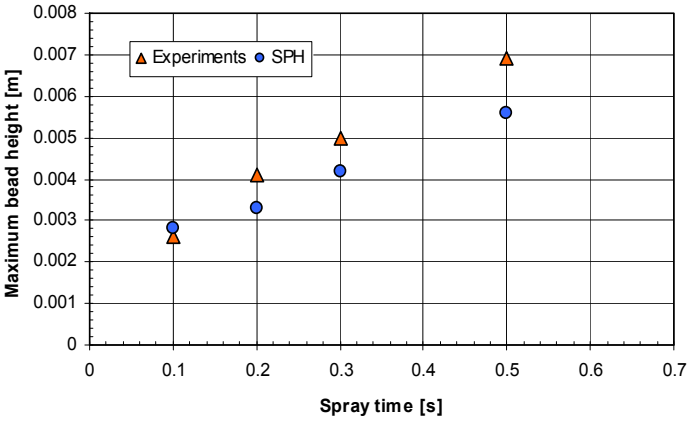

Figure 13: Bead height versus time, stationary applicator.

A snapshot from footage of the stationary applicator spraying high above the target plate is shown in Figure 11. From measuring the length of the black streaks, which in reality are sealing droplets, and from knowing the shutter time on the camera the injection velocity of the droplets was estimated to 10 m/s.

In Figures 12 and 13, results from the stationary applicator experiments and simulations are summarized. It can be seen that the width of the applied strings follow the experiments really well but that there is some discrepancy in the comparisons of bead height. When visually comparing the numerical and physical experiments, see Figures 3 and 14, the shape of the beads are matching. As both width and shape

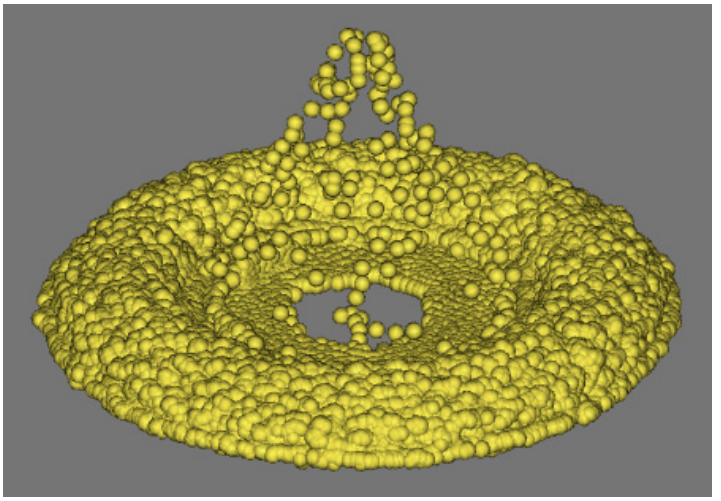

Figure 14: Simulated sealing application, using the same settings as in the case shown in Figure 3. Note the wall build-up of material surrounding an impact ditch, similar to what is seen in the physical experiments.

are similar there must be a discrepancy in bead volume, and as the SPH simulations are inherently mass conserving the only possible conclusion is that the volume of applied material in the experiments somehow is larger than in the simulations. As the mass of the applied material is the same in experiments and simulations there seems to be some entrainment of air as the sealing droplets impact the target, which possibly could make the material form a foam upon impacting the target. After cutting one of the larger beads open, small bubbles could be observed on the inside which possibly could support this hypothesis. Further, the hardened material is slightly elastic, which may also be an indication of a small scale spongy structure being present. A photo of the cut up material is shown in Figure 15.

In Figure 16, a rendition of a string application is shown together with photos from the experimental sessions. The similarity to the physical experiment with the same settings is striking. To quantitatively compare simulations to experiments, bead width as a function of applicator to target distance was measured and compared. The results are shown in Figure 17. As can be seen, for the shorter applicator to target distances the results coincide really well but in the case of larger distances the difference is increasing. One explanation for this may be that air-liquid interaction is completely disregarded in the simulations. This assumption holds true to a great extent as the transit time from applicator to target is small, but as the distance increases there is more time in which drag forces can act on the sealing material,

Figure 15: Photo of cut open sealing bead. Small cavities are visible to the naked eye.

reducing impact velocity and subsequently reducing the horizontal flow of material on the plate – thus giving a narrower bead. As the measurements of droplet velocity were rather crude, this hypothesis could not be verified using the measurement techniques available.

Surface tension would intuitively be thought to be of importance in this type of flow scenario. If, however, surface tension forces should be of relevance to the resulting shape of the formed bead the pressure drop over the surface interface should generate enough surface tension to balance gravity. That is, from Young-Laplace's equation we have

$$\Delta P_{surfacetension} = \frac{\gamma}{D} \approx \rho g D = \Delta P_{gravity} \tag{9}$$

Typical values of surface tension for a PVC sealer is around 30 mN/m and as the thickness of the strings are on the order of 5 mm we have for the left hand side of the expression $\Delta P_{surfacetension}$= 6 Pa and on the right hand side $\Delta P_{gravity}$ can be computed to 50 Pa, that is roughly a factor 10 larger pressure drop than the surface tension could generate. Thus, it must be the re-solidification of the sealing material rather than surface tension that prevents the bead from floating out more than it does.

The simulation time for the typical simulations of about two seconds of physical time was six hours using one processor on a Intel Core2 Quad CPU with 2.40GHz clock frequency and a time step of 10^{-6} s. The number of active SPH particles in these simulations were at maximum 10 000.

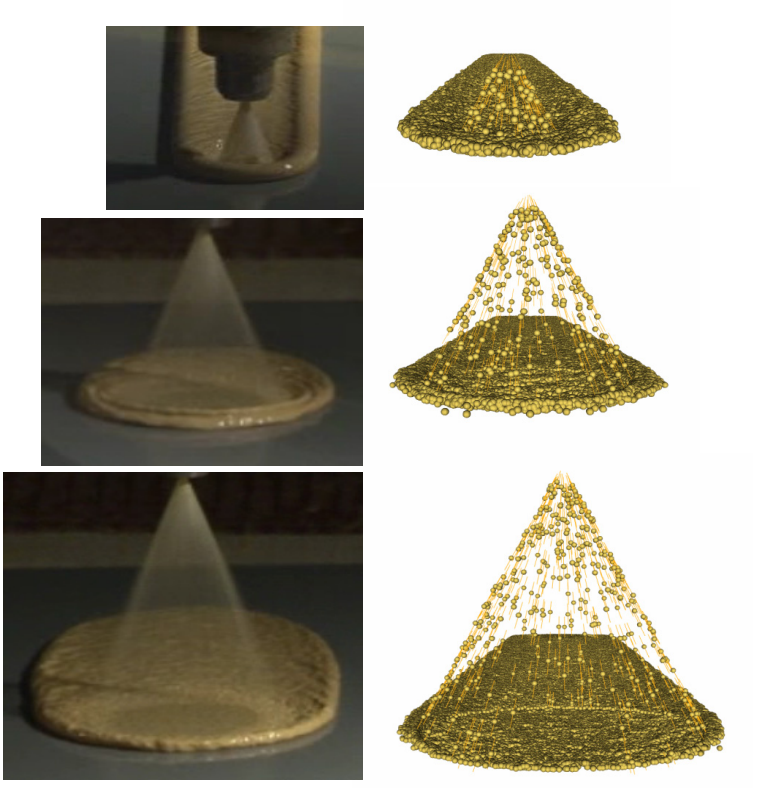

Figure 16: Comparison of experimental (left) and simulated (right) sealing application. Top, middle and bottom images show application of strings with applicator to plate distances of 20, 40 and 60 millimeters respectively.

5 Conclusions

Simulations and experiments of the process of applying sealing materials on car bodies have been performed. The results from the rotary rheometer experiments show that the sealing material behaves like a Bingham fluid, at least in the stationary limit. The results from the simulations show good agreement with the experiments using the hollowcone nozzle applicator. Although the work presented here only has

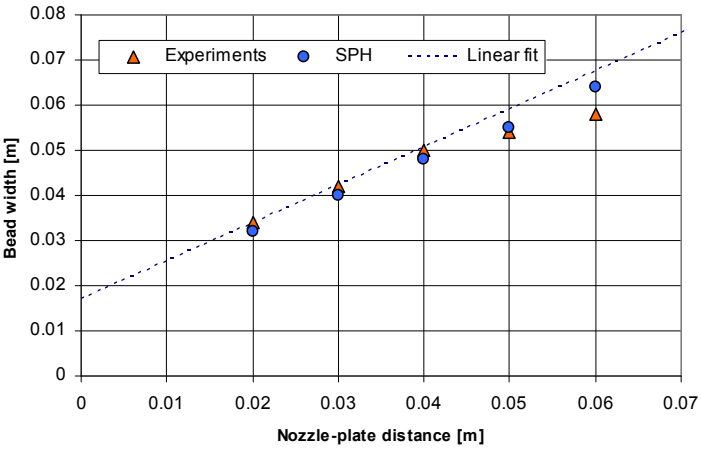

Figure 17: Bead width versus applicator to plate distance.

been concerned with the materials and applicators specific to the sealing process in a car paint shop the results and the methods are general and should apply to other (non turbulent) flow scenarios with other viscoelastic fluids.

Paint and surface treatment processes in automotive paintshops are very energy intensive and the increased demand on sustainability makes it necessary to further develop and optimize them. This research contributes to sustainable production by providing simulation tools that can be used by the automotive industry to reduce the time required for introduction of new car models, reduce the environmental impact and increase quality.

Acknowledgement: This work was supported in part by the Swedish Governmental Agency for Innovation Systems, VINNOVA, through the FFI Sustainable Production Technology program, and in part by the Sustainable Production Initiative and the Production Area of Advance at Chalmers. The support is gratefully acknowledged. The authors are also grateful for the valuable support of geometry models and experimental measurement data from our industrial collaborating partners Volvo Car Corporation and Saab Automobile AB.

References

Bingham, E.C. (1922): *Fluidity and Plasticity*, McGraw-Hill, New York, 1922.

Chorin, A.J. (1968): Numerical solution of the Navier-Stokes equations, *Math.*

Comput., vol. 22, pp. 745-762.

Cummins, S.J. and Rudman, M. (1999): An sph projection method. *J. Comp. Phys*, vol. 152, pp. 584-607.

Ellero, M. and Tanner, R.I. (2005): SPH simulations of transient viscoelastic flows at low Reynolds number, *J. Non-Newtonian Fluid Mech*, vol. 132, pp. 61-72.

Fang, J., Parriaux, A., Rentschler, M. and Ancey, C. (2009): Improved SPH methods for simulating free surface flows of viscous fluids, *Applied Numerical Mathematics*, vol. 59 no. 2, pp. 251-271.

Monaghan, J.J. (2005): Smoothed particle hydrodynamics, *Rep. Prog. Phys*., vol. 68, pp. 1703-1759.

Joseph P. Morris, J.P., Fox, P.J., and Zhu, Y. (1997): Modeling Low Reynolds Number Incompressible Flows Using SPH, *Journal of computational physics* vol. 136, pp. 214–22.

Rafiee, A., Manzari, M.T. and Hosseini, M. (2007): An incompressible SPH method for simulation of unsteady viscoelastic free-surface flows, *International Journal of Non-Linear Mechanics*, vol. 42, pp. 1210-1223.

Shao, S. and Lo, E.Y.M (2003): Incompressible SPH method for simulating Newtonian andnon-Newtonian flows with a free surface, *Advances in Water Resources,* vol. 26, pp. 787-800.

Tiwary, D. and Mehrota, A.K. (2004): Phase Transformation and Rheological Behaviour of Highly Paraffinic "Waxy" Mixtures, *The Canadian Journal of Chemical Engineering*, vol. 82, February.